Received: 6 February 2024 | Revised: 14 March 2024 | Accepted: 19 March 2024

DOI: 10.1111/jmi.13294

Journal of Microscopy RMS

THEMED ISSUE ARTICLE

Fluorescence microscopic investigation of PCE superplasticiser adsorption in calcined clay blended cement

D. Kosenko | **A. Wetzel** | **B. Middendorf**

Department of Structural Materials and Construction Chemistry, University of Kassel, Kassel, Germany

Correspondence
D. Kosenko, Department of Structural Materials and Construction Chemistry, University of Kassel, Mönchebergstr. 7, Kassel 34125, Germany.
Email: denis.kosenko@uni-kassel.de

Funding information
German Research Foundation (DFG), Grant/Award Number: 460294323

Abstract

Global efforts to minimise carbon dioxide emissions are also leading to attempts to use calcined clays (CC) as a partial substitute for cement in concrete. While the hydration mechanism of such CC blended cements is now well understood, the range of effective admixtures like polycarboxylate ethers (PCE) is limited. There are PCE types that promise relatively high effectiveness, but the mechanisms of action are not yet sufficiently understood. For a detailed understanding of the adsorption of such PCEs, spatially resolved studies of the binder were performed using a combination of fluorescence and scanning electron microscopy. In a comparison of two superplasticisers, the investigations have shown different sites of preferred adsorption in a CC blended system and the results can be correlated with flow tests and setting behaviour. The investigations have shown that a certain PCE type has a higher adsorption on CC and other components of a blended system in comparison to other types.

KEYWORDS

calcined clays, ESEM, fluorescence microscopy, fluorophores, light microscopy, particle fixation, PCE, staining, superimposition

1 | INTRODUCTION

As the production of cement clinker is currently responsible for approximately 8% of total annual worldwide CO_2 emissions[1] due to both the high temperatures required for the burning process and the chemical conversion of the raw material ($CaCO_3 \rightarrow CaO + CO_2$), efforts are being made to largely substitute Portland cement clinker (OPC) with materials of lower climate footprint. For this purpose, supplementary cementitious materials (SCM) can be used, such as granulated blast furnace slag, fly ash, silica fume or calcined clays.[2] Calcined clays (CC) are promising substitute materials, as the raw clays can be calcined at moderate temperatures of below 850°C[3] (compared to OPC, which must be burned at around 1450°C[4]) and do not release CO_2 through their own chemical conversion. CC blended cements show a sufficient strength development[5] and have a relatively high water demand[6] due to the high specific surface area and the platelet-like shape of the particles. In such blended systems, usually limestone and an additional sulphate carrier in the form of gypsum are also added.[7]

The demand for building materials such as concrete will increase worldwide,[8] this requires more durable and higher performance building materials in terms of climate compatibility. This higher performance is intended to extend the life cycle of buildings, which should

contribute to greater sustainability. There is already a range of purely cementitious high or ultra-high performance concretes (HPC and UHPC), which can meet the desired performance, but alternative or highly substituted systems are hardly found in this performance range.[9] The high performance of UHPC is achieved through a high packing density and low capillary porosity. In order to achieve this, the water to binder ratio (w/b) must mostly be set at relative low values between 0.20 and 0.30.[10] This is accomplished through the use of admixtures, typically polycarboxylate ethers (PCE), which are inadequate or ineffective in many alternative or highly CC-substituted systems.[11,12] PCEs consist of a polymer that has a 'comb structure' consisting of a chain of carboxyl groups, which are called backbone and polyether side chains extending from them. The synthesis of such polymers is performed by copolymerising the respective monomers for the backbone, for example acrylic acid, maleic anhydride or methacrylic acid, with the respective macromonomer for the side chain, for example α-allyl-ω-hydroxy poly(ethylene glycol) (APEG type PCE) or methoxy poly(ethylene glycol) methacrylate ester (MPEG type PCE).[12] In addition to such structures, there are also PCEs with other charge groups, which can also be cat- or zwitterionic, but they have so far played a subordinate role in the industry. The conventional PCEs have a similar mechanism of action; the carboxyl groups are deprotonated in the alkaline pore solution of a cement paste and therefore carry negative charges. The charge causes adsorption on positively charged particle surfaces, including the C_3A, C_4AF clinker phases as well as the early hydration product ettringite. By adsorbing on these surfaces, the positive charge is shielded on, so that there is a higher electrostatic repulsion between the particles due to the remaining negative charges. Additionally, there is a strong steric repulsion between the long side chains of the PCE, which together shows a strong dispersing effect on a cement paste.

It is known that the superplasticiser type is particularly important when using CC. Various studies have shown that the copolymer of acrylic acid as backbone monomer and α-methallyl-ω-hydroxy poly (ethylene glycol) ether as macro monomer (HPEG) has a high liquefaction effect in CC blended cements.[13–15] It is assumed that the higher effectiveness is due to a higher adsorption of the HPEG PCE on the CC.[12] Nevertheless, how the adsorption of a PCE is distributed in a finished blend of CC, limestone, sulphate carrier and OPC is difficult to measure indirectly (typically by total organic carbon or zeta potential measurements). Therefore, a microscopic approach should show how the adsorption of an HPEG is distributed in comparison with another APEG type PCE. Such approaches have been carried out in the past on pure fresh cement pastes. For example, fluorescence microscopy studies were performed on model particles (synthetic tobermorite, aluminium oxide, synthetic ettringite) and correlated with the zeta potential of the respective suspension.[16] In addition, studies were conducted on fresh pastes to track the retarding effect of various PCE superplasticisers.[17]

The methodical procedure described in Refs. 16 and 17 can be used in a modified form to visualise PCEs in a fluorescence microscope (FL) and to be able to follow the adsorption in spatial resolution. For this purpose, the PCE molecules are covalently coupled with a fluorescent marker (fluorophore) and analysed on a suitable preparation. By preparing the particles in the dry state, additional scanning electron microscope (SEM) images of the binder particles was taken in order to compare them with the fluorescence images.

2 | MATERIALS AND METHODS

2.1 | Powders and chemicals

To keep the system as simple as possible, pure raw materials were selected for the production of the pastes. The cement used should contain as few constituents as possible and should have a high clinker factor in order to determine on which clinker phases the respective PCE will primarily adsorb. For this reason, a white cement CEM I 42.5 from *Dyckerhoff* was chosen because of its high clinker content and because the clinker consisted only of tricalcium silicate alite (C_3S, Ca_3SiO_5), dicalcium silicate belite (C_2S, Ca_2SiO_4) and tricalcium aluminate (C_3A, $Ca_3Al_2O_6$) and contained no aluminoferrite phase (C_4AF, $Ca_2(Al,Fe)_2O_5$). The second largest mass fraction in the binder mixture was made up of CC; *Metastar 501 HP* from *Imerys* with a high metakaolin content was used for this purpose. This material had a high degree of purity and a high amorphous content. The product *Kalksteinfüller KSF 60/3* from *Fels-Werke GmbH* was used as limestone powder. It is a commercial product approved for use as a concrete additive in self-compacting concrete. Hemihydrate can be used as a sulphate source in such systems; stucco from *Knauf* was used for this purpose. The material was a gypsum binder A1 according to EN 13279-1. According to the data sheet, the proportion of organic components was less than 1%.

2.2 | Sample preparation

Pastes of a limestone, calcined clay and Portland cement were produced, with a content of 50% of Portland cement. The w/b was kept constant at 0.50 and the PCE content is set to 1% by weight of binder (bwob). Table 1 shows

TABLE 1 Composition of the used paste for microscopy.

Component	Percentage (%)	Weight (mg)
Calcined clay	30	105
Hemihydrate	5	17.5
Limestone	15	52.5
Cement	50	175
Stained PCE	1 (bwob)	3.5
Water	–	175

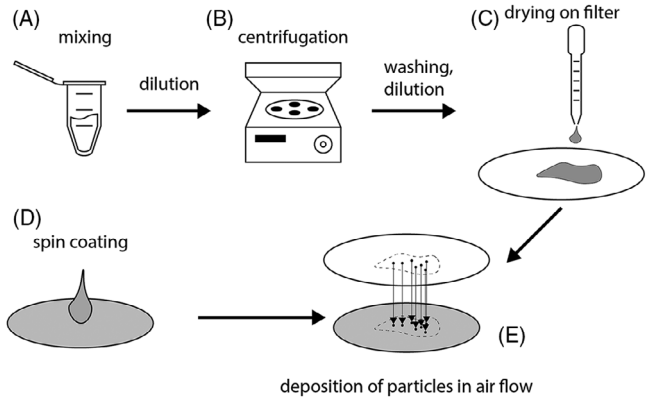

FIGURE 1 Preparation of samples for microscopy from a defined paste.

the composition of the dry substances and the resulting weights for one sample vessel.

For microscopic examination, this firmly defined paste should reflect the distribution of the PCE. Methodologically, this cannot be accomplished using the above-mentioned, existing setup[17,18] because the particles are placed in a suspension on a microscope slide. To achieve the required particle separation, the fine fraction of the powder had to be separated and the *w*/*b* had to be adjusted to 5 in these publications. To overcome this disadvantage and to bring the *w*/*b* to that of a real binder system like shown in Table 1, the particles and the PCE must be separated from the pore solution and fixed on a suitable support for microscopy. This can be accomplished by centrifugation and repeated washing of the supernatant from the binder particles. Consideration should be given as to whether, and in what time frame, significant desorption of PCE from the particles will occur. Previous studies on solid particles using the method of Arend et al.[18] combined with the steps **C**, **D** and **E** shown in Figure 1 have shown that washing off a PCE with deionised water cannot be measured on both inert and reactive particles over an extended period of time. Therefore, the method was expanded to include steps **A** and **B** in order to separate the PCE-occupied particles from the liquid; the experiments were already able to provide high-resolution images of the PCE distribution on pure white cement.[19]

To prepare the samples, the dry substances shown in Table 1 were weighed into a vessel. The PCE was dissolved in water in a second vessel. After the PCE has completely dissolved, the liquid was mixed with the dry substances in a vortex mixer like shown in Figure 1, step **A**. The mixture was left to rest for 15 min with occasional mixing, then 5 mL of water were added and centrifuged at 3000 rpm for 5 min (step **B**). The procedure was repeated. A last wash cycle was carried out with 5 mL isopropanol. The particles were dispersed again in 5 mL isopropanol, picked up with a pipette and 10 drops are dripped onto a filter (step **C**). After drying, the powder was transferred in a stream of air to a glass surface freshly spin-coated with *M-glass* (Merck) like shown by step **E**. Spin coating (step **D**) was performed by dropping the liquid film onto a cutted microscope slide and rotating at 5000 rpm for 2 s.

2.3 | Superplasticisers and staining

PCEs of HPEG and APEG type were obtained from Prof. Plank's group at the Department of Chemistry at the TU Munich. In order to observe the PCEs in a fluorescence microscopic measurement, a staining reaction was performed. This reaction involves attaching a fluorophore, Rhodamine B (Rhod B), to a PCE molecule through a covalent bond. The reaction involves the formation of a reactive intermediate from the PCE using 1-Ethyl-3-(3-dimethylaminopropyl)carbodiimide (EDC) and *N*-hydroxysuccinimide (NHS). The intermediate can then couple with Rhod B to produce a fluorescent PCE-marker molecule by using ethylenediamine (EDA) as a linker molecule. The synthesis is carried out like shown in Figure 2 out in two steps, Rhod B (**1**) has a carboxyl group that can be activated with EDC and NHS to form a reactive NHS ester with Rhod B (**2**).[20] Analogously, the respective PCE (**3**) can be activated in parallel with EDC and NHS in order to be able to covalently bind with a primary amine of the EDA molecule (**4**) while still in the solution. The product (**5**) of this reaction step is a molecule in which the PCE is connected to the EDA by an amide bond. The products of the two partial reactions can also be linked with the same reaction; the amine group of the PCE-EDA intermediate (**5**) is covalently bound to the activated Rhod B (**2**). The product is a PCE molecule attached to the Rhod B fluorophore via two amide groups and two carbon atoms (**6**). During the reaction, a by-product urea species is formed. In each of the three partial reactions, the EDC is oxidised by a carbodiimide to a urea; NHS has a catalytic effect. This by-product, catalyst and unreacted educts can be separated from the desired product through dialysis due to its large difference in molar mass compared to the PCE (EDC = 155.24 g/mol, NHS = 115.09 g/mol, EDA = 60.1 g/mol, Rhod

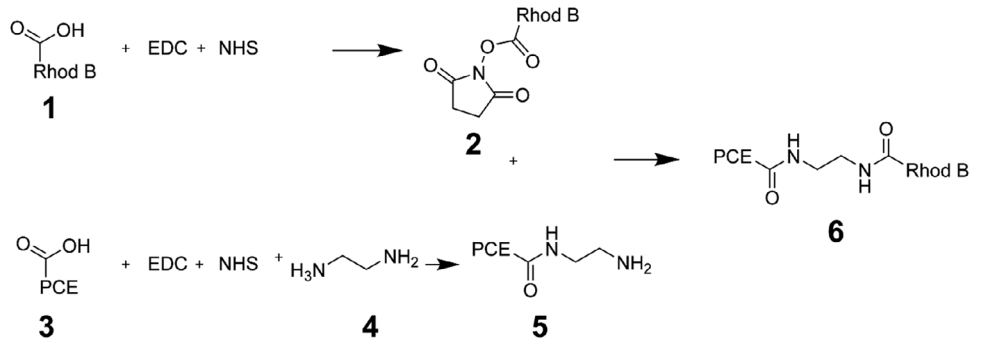

FIGURE 2 Staining of a PCE with Rhodamine B.

B = 479.02 g/mol). Figure 2 illustrates the combination of the reactants.

The staining reaction was carried out as follows: 4 g calculated from the respective solid content of the PCE were given into a flask and filled up to 48 g. 28.8 mg (1.5×10^{-4} mol) EDC and 6.9 mg (6×10^{-5} mol) NHS were dissolved in 1 mL 2-(*N*-morpholino)ethanesulphonic acid (MES) buffer solution and given to the solution. 20 µL (18 mg, 3×10^{-4} mol) EDA was given to the solution. In a vial, 14.4 mg (3×10^{-5} mol) Rhod B, 5.8 mg (3×10^{-5} mol) EDC and 6.9 mg (3×10^{-5} mol) NHS were dissolved in 2 mL MES buffer and stirred for 2 h at room temperature. After stirring, the mixture from the vial was given into the flask and stirred for 5 days at room temperature. After stirring, the mixture was given into a dialysis tube with a molecular weight cutoff (MWCO) of 3.5 kDa and fixed with locking clamps. The filled dialysis tube was fixed in a 5 L bucket, filled up to 4.5 L and stirred for 5 days with everyday water exchange. After 4 days, the dialysis water was clear.

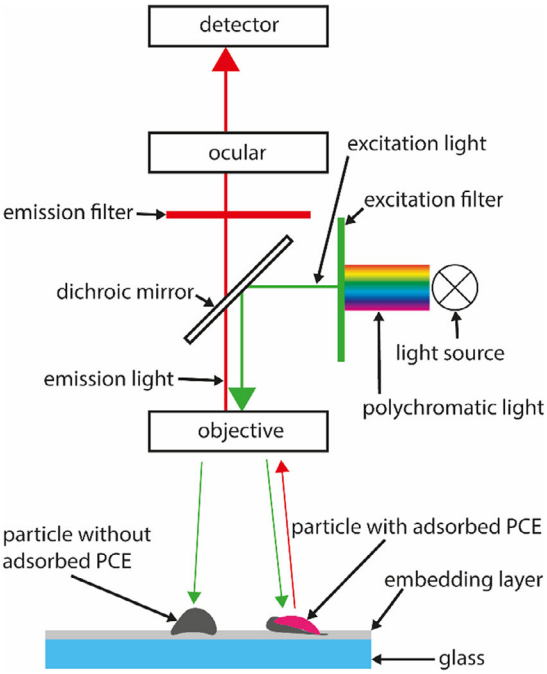

FIGURE 3 Fluorescence microscopy applied on fixed particles with adsorbed fluorescent PCE.

2.4 | Fluorescence microscopy

The fluorescence images were taken with a Leica M 205 MA microscope on fixed particles like schematically shown in Figure 3. A bandpass filter with wavelengths of 525–560 nm (green light) was used for excitation and a bandpass filter with 590–650 nm (red light) for emission. The exposure time was set to 5 s at maximum intensity. The substrate produced in Section 2.2 was therefore a microscope slide with fixed particles on it. Centrifugation and washing in turn results in the particles being covered with the respective fluorescent PCE. As shown in Figure 3, the fluorescence signal is only emitted by the PCE molecules, which means that only these are visible in fluorescence mode. In order to obtain a comparison with the localisation of the particles, reflected light images are recorded.

A light source emits polychromatic light, and a bandpass filter (indicated in green) is used to filter out only the desired excitation wavelength. The excitation light is then initiated into the lens system of the microscope using a dichroic mirror (in this case, a low pass filter that reflects frequencies over the cutoff frequency). After the sample is excited, the objective collects the emitted light from the sample, which has a higher wavelength than the exciting light (indicated in red). The collected light passes through the dichroic mirror, emission filter and ocular before being detected. The emission filter is necessary because the emitted light is not monochromatic. Typically, the emitted light consists of a spectrum of all wavelengths higher than the excitation wavelength, so the wave band of interest must be filtered out before reaching the detector.

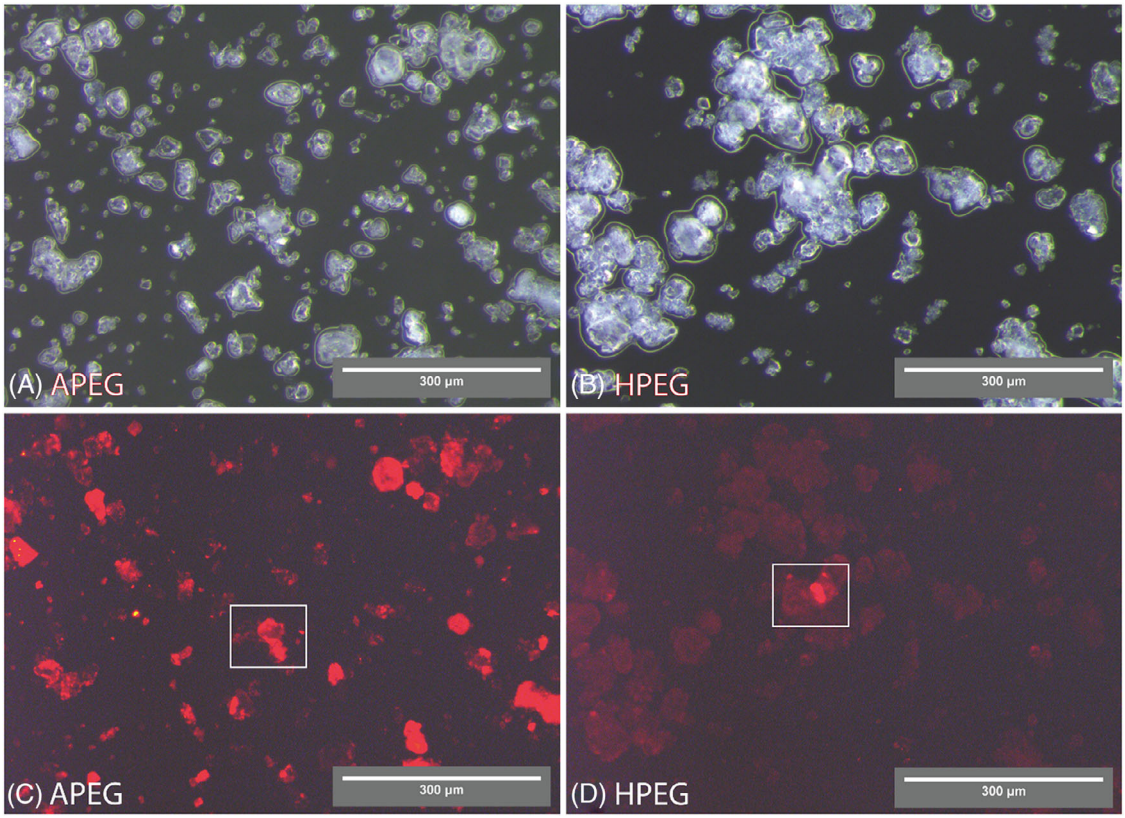

FIGURE 4 Reflected (A, B) and adjusted fluorescent light images (C, D) of the particles (equivalently brightened).

2.5 | ESEM

The samples were analysed using ESEM. Measurements were made on a FEI QUANTA 250 FEG ESEM with a voltage of 15 kV and a vacuum of approximately 5×10^{-2} mbar. Acquisitions were made in backscattered electron (BSE) mode of the raw materials and the samples of the binder. Images of the raw materials and samples of the binder were taken in order to be able to compare the substances in the samples. With the ESEM images of the samples obtained, the fluorescence images are to be used to determine which particles the respective PCE adsorb on.

2.6 | Fresh concrete properties

In addition to the fundamental microscopic investigations, the effects of PCEs on the fresh and hardened concrete properties are also of great interest for further applications. Therefore, the flowability of the resulting pastes was tested using a 'mini-slump' test derived from DIN EN 1015-3 in which the dimensions of the slump funnel were halved. These small dimensions were chosen due to the limited availability of the respective PCE.

3 | RESULTS

3.1 | Fluorescence images

The reflected light images were used to determine the particle localisation on the samples. A first look showed a different distribution of the particles on the samples. This is due to the preparation method, which is difficult to control because the distribution of particles on the surface cannot be controlled by the airflow like shown in Figure 1, step **E**. In addition, precise control of the part coverage on the filter in step **C** has been inadequate. However, the distribution of fluorescence intensity between samples with HPEG and APEG differs significantly. Here it can be recognised for APEG that the fluorescence on certain particles is strongly increased while other particles are hardly visible or not visible at all (comparison of Figure 4A and C). If the comparison is made for a sample with HPEG (Figure 4B and D), although the fluorescence intensity does not have such high peak values as with APEG, it appears to be uniformly distributed over the entire material.

If the fluorescence signal is assumed to be representative of the coverage of the particles with the respective

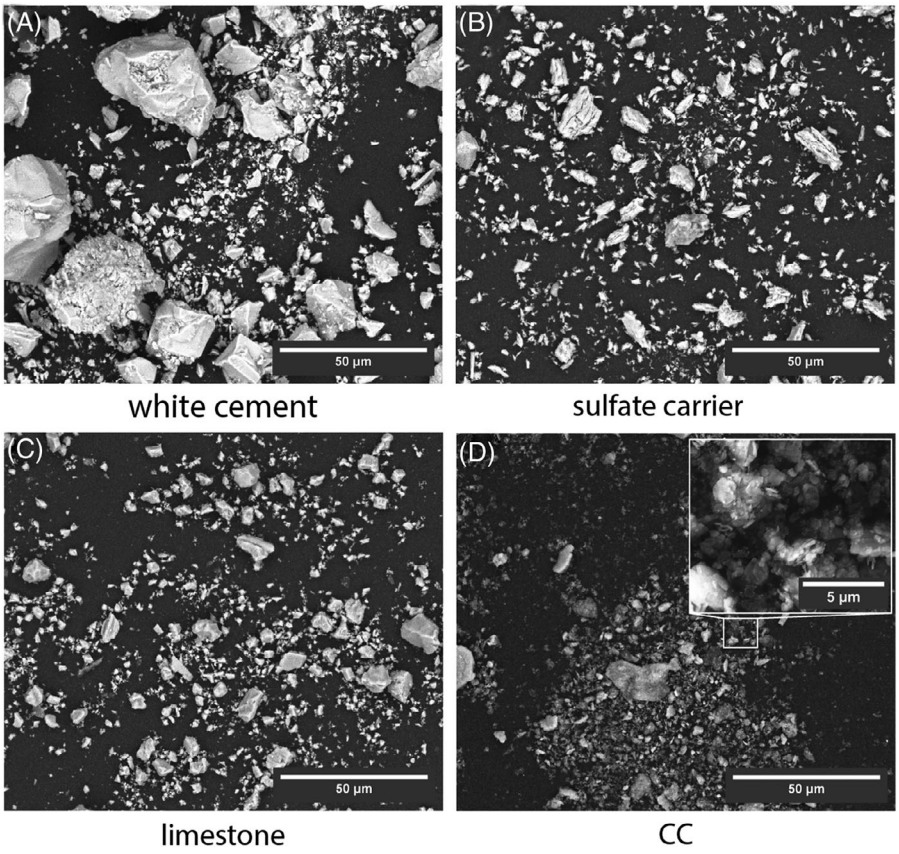

FIGURE 5 ESEM pictures of the raw materials for production of the pastes.

PCE, the distribution of HPEG is uniform while APEG favours certain locations. It can be seen from the images that the intensities differ between the two PCEs. This is due to the different molar masses of the PCEs, since the same mass of both PCEs was used for the staining reaction. This results in a different number of stained -COOH groups, which changes the absolute intensity values. This circumstance does not allow a comparison of the absolute adsorption values of the two PCEs. Because there is no quantitative comparison, but a determination of the preferred adsorption sites on the particles, this circumstance can be neglected for the evaluation.

3.2 | Comparison between ESEM and fluorescence results

ESEM images were taken and compared with the fluorescence images obtained to visualise the surfaces on which the respective PCE is adsorbed. The measurements were performed in BSE mode to distinguish the particles morphologically based on the particle shape. For this purpose, the morphology of the raw materials, shown in Figure 5, is compared with the products obtained. Since white cement is a finished product, there is a small number of other ingredients in the mix in addition to clinker like sulphate carrier. The material shown in Figure 5A represents clinker particles of different sizes. Distinguishing between the sulphate carrier mostly consisting of hemihydrate (Figure 5B) and limestone (Figure 5C) presents a greater challenge due to their similar morphology. CC is relatively well to identify due to their flat morphology, as shown in Figure 5D.

Figure 6 shows the white marked area of the taken fluorescence images of the samples shown in Figure 4D. The ESEM image in Figure 6A shows agglomerates of CC, limestone, ettringite and not dissolved calcium silicate phases which were marked with different colours. Figure 6B, on the other hand, shows the pure fluorescence signal from the marked section. A superimposition of both images shows the distribution of the FL signal on the respective particles as shown in Figure 6C. In the superimposition can be seen that the HPEG appears to be evenly distributed across most components of the mixture. Deviations in the distribution can be found on the supposed ettringite-rich area marked in the image in purple, where adsorption is highest, and on the supposed limestone marked in blue, where it is lowest. For better visualisation, the area of the fluorescence signal in Figure 6C is framed in blue.

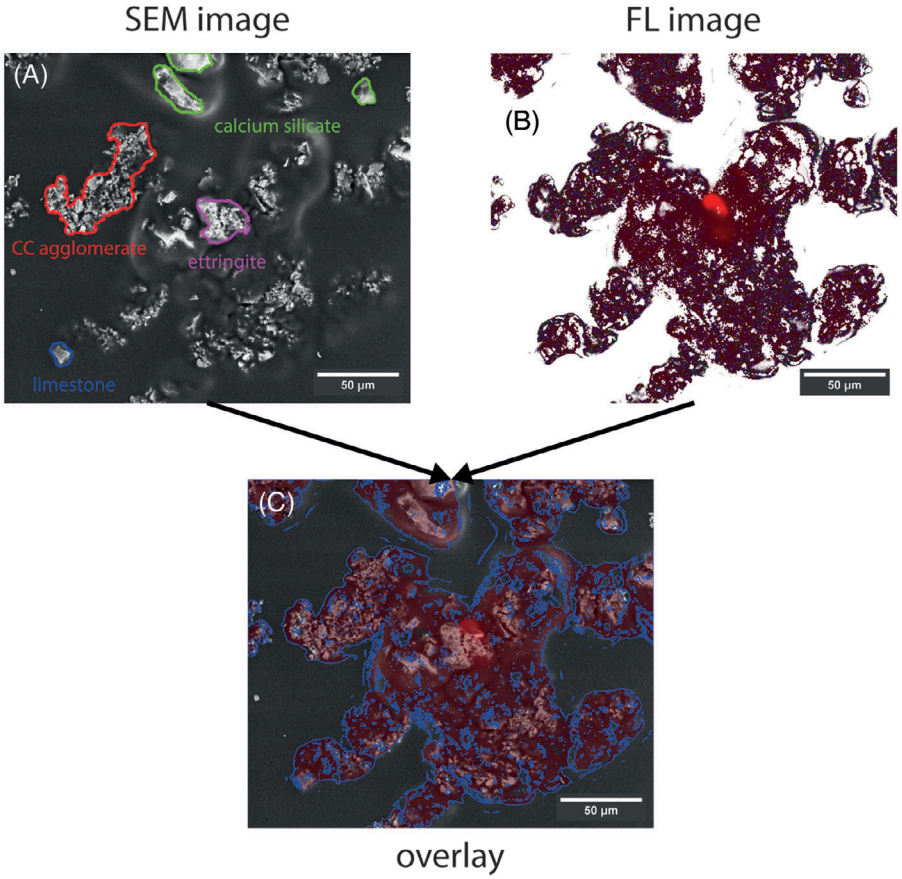

FIGURE 6 ESEM-BSE image (A), fluorescence image (B) and superimposition of BSE with the fluorescence signal of HPEG (C).

In contrast to the uniform distribution of HPEG, APEG shows a high spatial dependence of adsorption. Figure 7 shows the marked area of the fluorescence image Figure 4C. Larger calcium silicate phases surrounded by assumed ettringite-rich agglomerates of CC, limestone and gypsum can be recognised, which can be recognised by the coloured markings in Figure 7A. In comparison, the superimposition of the ESEM-BSE image and the FL-image (Figure 7B) in Figure 7C shows that the adsorption of APEG on ettringite appears to be favoured. The biggest difference to the HPEG samples is that the difference between the adsorption at these favoured sites and the nonfavoured sites is relatively large.

From the ESEM and FL images, it can be seen that HPEG shows a wide distribution on different components of a blended binder system. A comparison of the areas identified from the raw materials for the different components of the system shows that the adsorption on ettringite is increased, but there is also significant adsorption on alite, belite and CC.

APEG, on the other hand, is primarily due to the ettringite formed or possibly the tricalcium aluminate that has not totally yet dissolved underneath. It has little or no affinity for the other components of the mixture.

3.3 | Flowability

The mixture from Table 1 was scaled up to obtain a mixture volume of 50 mL; the w/b was lowered to 0.30 and stirred for 2 min with a hand mixer. With the deliberately low w/b selected, the paste without PCE was not flowable, so a value of 5 cm was selected to describe the spread flow based on the dimensions of the outlet cone. Figure 8D shows the obtained pastes with the respective spread flow values. Without superplasticiser, the material is earth moist (Figure 8A); with APEG (Figure 8B), a plastic paste is created, which has an extremely low flowability. When using HPEG (Figure 8C), an enormous liquefaction effect can be seen, so that the material runs very unevenly.

4 | DISCUSSION

The superimposition of the fluorescence images with the ESEM images shows that the adsorption of HPEG and APEG on the paste of a CC-substituted cement differs. The adsorption of the HPEG PCE used shows less extreme preference for one of the components of the mixture compared to APEG. There is an increased adsorption on ettringite,

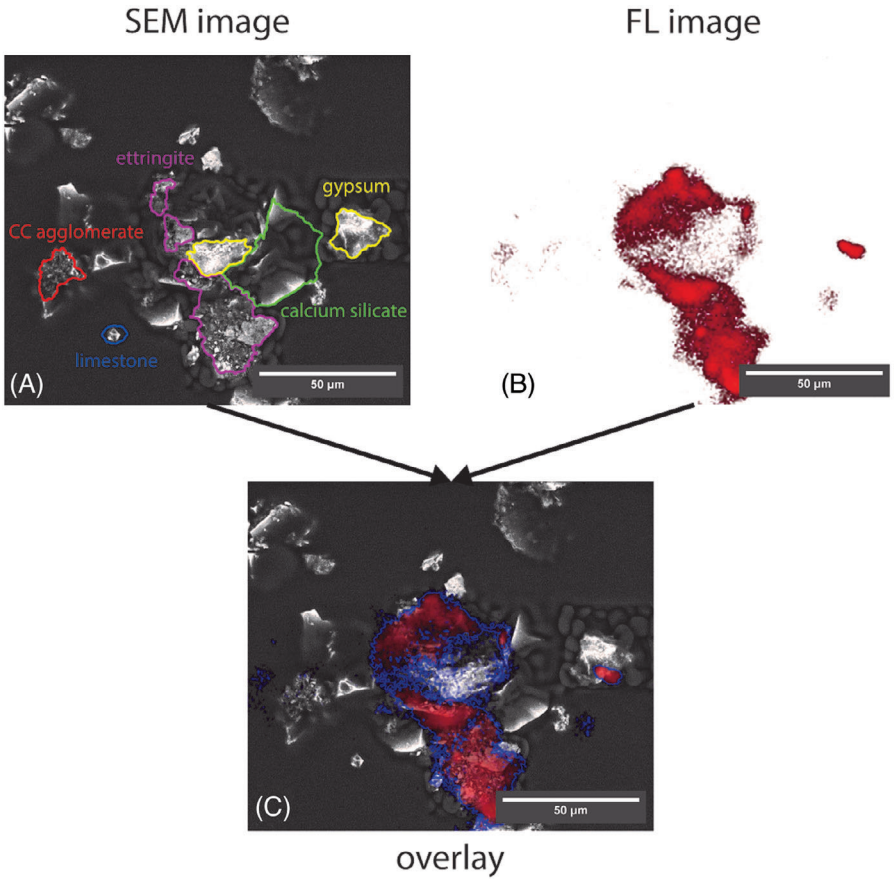

FIGURE 7 ESEM-BSE image (A), fluorescence image (B) and superimposition of BSE with the fluorescence signal of APEG (C).

but the adsorption on C_3S, C_2S and CC is also increased in relation to the maximum value. Based on the images obtained, no more precise information can be given about the adsorption of HPEG on limestone or gypsum, since the measured areas did not contain sufficient particles of these components.

It can therefore be stated that the HPEG PCE has an increased adsorption on CC, limestone and the sulphate phases, which leads to an improved liquefaction effect. However, given the small structural difference between the two PCEs used, the reason for this behaviour cannot be mechanistically explained. It can be stated that the dialysis washed out any unreacted monomers contained in the copolymerisation during the staining process, so that the higher liquefaction effect can actually be attributed to the type of PCE and not to unwanted components in the polymer. The HPEG PCE used is a molecule with relatively long side chains. The side chains of polyethylene glycol (PEG) are known to have a chelating effect on alkali and alkaline earth metals similar to that of crown ethers.[21] It is known that the side chains can receive a positive charge from the ions they contain,[22] thereby become bifunctional[23] and therefore adsorb on the negatively charged calcium silicate phases and CC in the observed system.

APEG seems to attach primarily to the C_3A phase and allegedly on the rapidly forming ettringite on it, which often contains the other components to which APEG seems to attach only marginally. The results from the fluorescence microscopic measurements therefore correlate with the measured flow properties of the pastes. A possible explanation for the behaviour of the APEG superplasticiser lies in the general competitive adsorption between SO_4^{2-} ions and PCEs on ettringite.[24] If the formation of ettringite is formed by dissolved C_3A and sulphate ions in the solution, then dissolved Ca^{2+} ions from the C_3A phase are a starting material for the precipitation reaction. However, APEG is known to have a high chelating effect for Ca^{2+} ions due to maleic anhydride as backbone monomer.[25] The idea is therefore that APEG must have a high affinity for tricalcium aluminate and ettringite. Previous studies comparing APEG with other PCE types have also shown this retarding effect and prevention of early hydration products.[17] These studies have shown that APEG forms a barrier layer so that water is prevented from reaching the cementitious phases. This also led to a delay of several weeks in C_3S hydration.[18] However, the presented study here only looks at a time point shortly after mixing.

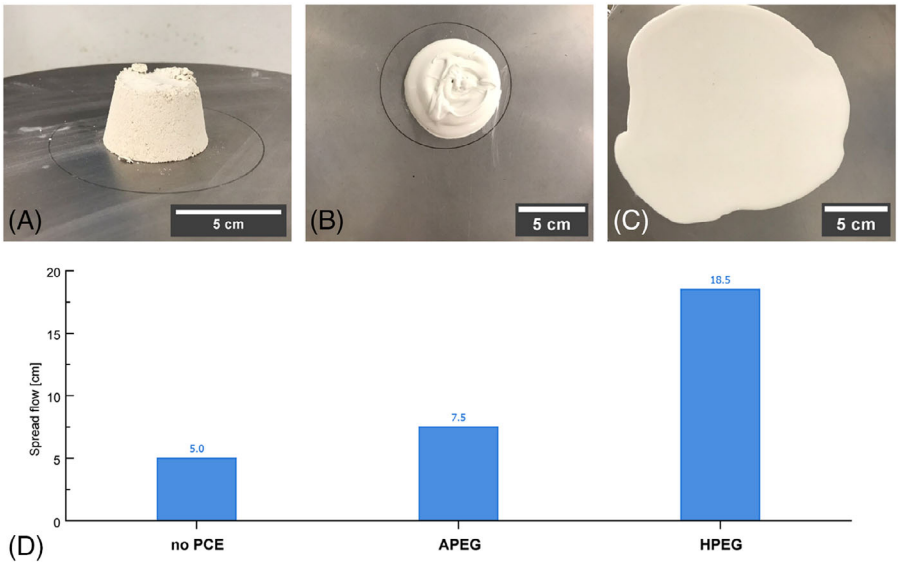

FIGURE 8 Resulting pastes and measured spread flow values.

Summarising, the flowability of mixes containing APEG is lower than for HPEG at the same dosage.

5 | CONCLUSION AND OUTLOOK

The following statements can be made based on fluorescence images, ESEM images and flow tests:

a. For the selected system made of white cement, CC, limestone and sulphate carrier, a high liquefaction effect was observed with a HPEG superplasticiser, while an APEG superplasticiser used only showed a marginal effect.
b. The fluorescence microscopy images show a very different distribution for the two PCEs. This shows that HPEG is more widely distributed on the particles while APEG favours certain areas.
c. Comparing ESEM, light and fluorescence microscopy can be used to determine which phases and surfaces PCE prefers to adhere to.
d. The microscopic results correlate with the measured macroscopic material properties.

The work shown here also raises further questions regarding both the preparation method and the results obtained. Methodologically, there is still a need for optimisation in terms of particle distribution and fixation, as the film used seems to partially creep onto the surface of the particles to be analysed, which makes the evaluation more difficult. The solution can be achieved by further adjusting the spin coating and deposition steps. The retardation effect caused by APEG can be observed by time-dependent measurements; coupling with ESEM allows a precise analysis of the educts as well as the products and the adsorption of PCE on them. In a further step, the samples can potentially be used to study the desorption of the respective sample in the presence of sulphate ions in more detail.

ACKNOWLEDGEMENTS

This project is funded by the German Research Foundation (DFG), grant number 460294323. The authors thank Prof. Plank, Department of Chemistry at the TU Munich, for providing the PCEs.

Open access funding enabled and organized by Projekt DEAL.

ORCID

D. Kosenko https://orcid.org/0000-0003-1362-2645
A. Wetzel https://orcid.org/0000-0003-2680-9708

REFERENCES

1. Sousa, V., Bogas, J. A., Real, S., Meireles, I., & Carriço, A. (2023). Recycled cement production energy consumption optimization. *Sustainable Chemistry and Pharmacy*, *32*, 101010.
2. Lothenbach, B., Scrivener, K., & Hooton, R. D. (2011). Supplementary cementitious materials. *Cement and Concrete Research*, *41*(12), 1244–1256.
3. Hanein, T., Thienel, K.-C., Zunino, F., Marsh, A. T. M., Maier, M., Wang, B., Canut, M., Juenger, M. C. G., Ben Haha, M., Avet, F., Parashar, A., Al-Jaberi, L. A., Almenares-Reyes, R. S., Alujas-Diaz, A., Scrivener, K. L., Bernal, S. A., Provis, J. L., Sui, T., Bishnoi, S., & Martirena-Hernández, F. (2022). Clay calcination technology: State-of-the-art review by the RILEM TC 282-CCL. *Materials and Structures*, *55*(3), 1–29.
4. Ludwig, H.-M., & Zhang, W. (2015). Research review of cement clinker chemistry. *Cement and Concrete Research*, *78*, 24–37.

5. Sharma, M., Bishnoi, S., Martirena, F., & Scrivener, K. (2021). Limestone calcined clay cement and concrete: A state-of-the-art review. *Cement and Concrete Research*, *149*, 106564.
6. Py, L. G, Neto, J. S. A, Longhi, M. A, & Kirchheim, A. P. (2024). Evaluation of ultrafine calcined clays on LC3 cements on the sulfate requirement, water demand and strength development. *Materials and Structures*, *57*(1), 1–16.
7. Zunino, F., & Scrivener, K. L. (2023). Recent advances in understanding the hydration of limestone calcined clay cements (LC3). Further Reduction of CO2-Emissions and Circularity in the Cement and Concrete Industry, 16th International Congress on the Chemistry of Cement 2023 – ICCC2023. Thailand Concrete Association. https://doi.org/10.3929/ETHZ-B-000636037
8. Uratani, J. M, & Griffiths, S. (2023). A forward looking perspective on the cement and concrete industry: Implications of growth and development in the Global South. *Energy Research & Social Science*, *97*, 102972.
9. Glanz, D., Sameer, H., Göbel, D., Wetzel, A., Middendorf, B., Mostert, C., & Bringezu, S. (2023). Comparative environmental footprint analysis of ultra-high performance concrete using portland cement and alkali-activated materials. *Frontiers in Built Environment*, *9*, 86.
10. An, M., Liu, Y., Zhang, G., & Wang, Y. (2023). Properties of cement-based materials with low water–binder ratios and evaluation mechanism under further hydration effect. *Applied Sciences*, *13*, 9964.
11. de Hita, M. J., & Criado, M. (2023). Influence of superplasticizers on the workability and mechanical development of binary and ternary blended cement and alkali-activated cement. *Construction and Building Materials*, *366*, 130272.
12. Lei, L., Hirata, T., & Plank, J. (2022). 40 years of PCE superplasticizers – History, current state-of-the-art and an outlook. *Cement and Concrete Research*, *157*, 106826.
13. Li, R., Lei, L., Sui, T., & Plank, J. (2021). Effectiveness of PCE superplasticizers in calcined clay blended cements. *Cement and Concrete Research*, *141*, 106334.
14. Li, R., Lei, L., & Plank, J. (2022). Impact of metakaolin content and fineness on the behavior of calcined clay blended cements admixed with HPEG PCE superplasticizer. *Cement and Concrete Composites*, *133*, 104654.
15. Schmid, M., & Plank, J. (2020). Dispersing performance of different kinds of polycarboxylate (PCE) superplasticizers in cement blended with a calcined clay. *Construction and Building Materials*, *258*, 119576.
16. Arend, J., Wetzel, A., & Middendorf, B. (2018). In-situ investigation of superplasticizers: From fluorescence microscopy to concrete rheology. *Cement and Concrete Research*, *113*, 178–185.
17. Arend, J., Wetzel, A., & Middendorf, B. (2020). Fluorescence microscopic investigations of the retarding effect of superplasticizers in cementitious systems of UHPC. *Materials (Basel, Switzerland)*, *13*(5), 1–13.
18. Arend, J., Wetzel, A., & Middendorf, B. (2020). Fluorescence microscopy of superplasticizers in cementitious systems: Applications and challenges. *Materials (Basel, Switzerland)*, *13*(17), 3733.
19. Kosenko, D., Wetzel, A., & Middendorf, B. (2023). Spatially resolved in situ analyses of the adsorption behavior of different admixtures on binders. *ce/papers – Proceedings in Civil Engineering*, *6*(6), 477–483.
20. Tsakos, M., Schaffert, E. S., Clement, L. L., Villadsen, N. L., & Poulsen, T. B. (2015). Ester coupling reactions – An enduring challenge in the chemical synthesis of bioactive natural products. *Natural Product Reports*, *32*(4), 605–632.
21. Fenton, D. E., Parker, J. M., & Wright, P. V. (1973). Complexes of alkali metal ions with poly(ethylene oxide). *Polymer*, *14*(11), 589.
22. Zhivkova, I. V., Zhivkov, A. M., & Stoychev, D. S. (1998). Electroctatic bahviour of polyethylene oxide. *European Polymer Journal*, *34*(3/4), 531–538.
23. Wu, B., Chun, B.-W., Gu, L., & Kuhl, T. L. (2018). Effect of Ca2+ ion concentration on adsorption of poly(carboxylate ether)-based (PCE) superplasticizer on mica. *Journal of Colloid and Interface Science*, *527*, 195–201.
24. Schmidt, W., Brouwers, H. J. H., Kühne, H.-C., & Meng, B. (2013). Optimierung der Robustheit von selbstverdichtendem Beton gegenüber Temperatureinflüssen. *Beton und Stahlbetonbau*, *108*(1), 13–21.
25. Conte, T., & Plank, J. (2019). Impact of molecular structure and composition of polycarboxylate comb polymers on the flow properties of alkali-activated slag. *Cement and Concrete Research*, *116*, 95–101.

How to cite this article: Kosenko, D., Wetzel, A., & Middendorf, B. (2024). Fluorescence microscopic investigation of PCE superplasticiser adsorption in calcined clay blended cement. *Journal of Microscopy*, *294*, 215–224. https://doi.org/10.1111/jmi.13294